Pure visual imagery as a potential approach to achieve three classes of control for implementation of BCI in non-motor disorders

Pure visual imagery as a potential approach to achieve three classes of control for implementation of BCI in non-motor disorders

Teresa Sousa[1,2,3], Carlos Amaral[1], João Andrade[1], Gabriel Pires[3], Urbano Nunes[3], Miguel Castelo-Branco[1,2]

[1] Institute for Biomedical Imaging and Life Sciences (CNC.IBILI), Faculty of Medicine, University of Coimbra, Coimbra, Portugal.

[2] Institute of Nuclear Sciences Applied to Health (ICNAS), University of Coimbra, Coimbra, Portugal

[3] Institute of Systems and Robotics (ISR-UC), Department of Electrical and Computer Engineering, University of Coimbra, Coimbra, Portugal.

Abstract

Objective: The achievement of multiple instances of control with the same type of mental strategy represents a way to improve flexibility of BCI systems. Here we test the hypothesis that pure visual motion imagery of an external actuator can be used as a tool to achieve three classes of EEG based control, which might be useful in attention disorders.

Approach: We hypothesize that different number of imagined motion alternations lead to distinctive signals, as predicted by distinct motion patterns. Accordingly, distinct number of alternating sensory/perceptual signals would lead to distinct neural responses as previously demonstrated using fMRI. We anticipate that differential modulations should also be observed in the EEG domain. EEG recordings were obtained from twelve participants using three imagery tasks: imagery of a static dot, imagery of a dot with two opposing motions in the vertical axis (2 motion directions) and imagery of a dot with four opposing motions in vertical or horizontal axes (4 directions). The data were analysed offline.

Main results: An increase of alpha-band power was found in frontal and central channels as a result of visual motion imagery tasks when compared with static dot imagery, in contrast with the expected posterior alpha decreases found during simple visual stimulation. The successful classification and discrimination between the three imagery tasks confirmed that three different classes of control based on visual motion imagery can be achieved. The classification approach was based on SVM and on the alpha-band relative spectral power of a small group of six frontal and central channels. Patterns of alpha activity, as captured by single-trial SVM closely reflected imagery properties, in particular the number of imagined motion alternations.

Significance: We found a new mental task based on visual motion imagery with potential for the implementation of multiclass (3) BCIs. Our results are consistent with the notion that frontal alpha synchronization is related with high internal processing demands, changing with the number of alternation levels during imagery. Together, these findings suggest the feasibility of pure visual motion imagery tasks as a strategy to achieve multiclass control systems with potential for BCI and in particular neurofeedback applications in non-motor (attentional) disorders.

Keywords: Multiclass control, visual motion imagery.

Introduction

Current neuroimaging technologies allow to investigate the neural correlates of perceptual operations. A deep understanding of such correlates may help design neural interfaces that use such signals in brain-computer interfaces (BCI) or neurofeedback approaches. In some non-motor diseases such as attentional disorders, self-centered state control, used in the more specific context of neurofeedback (Banca *et al* 2015, DeBettencourt *et al* 2015, Ordikhani-Seyedlar *et al* 2016), is more important than speed of communication (as used in motor BCIs).

BCI approaches measure and convert brain signals into artificial outputs (Farwell and Donchin 1988, Wolpaw and McFarland 2004). These systems enable users to act on the world by using their brain signals rather than the brain's normal output pathways of peripheral nerves and muscles (Shih *et al* 2012). BCI systems can be applied as assistive BCIs or as neurofeedback approaches (Chaudhary *et al* 2016). Assistive BCIs aim to support the daily life of users with deficits of for example in motor or communication functions (McFarland and Wolpaw 2011). On the other hand, neurofeedback systems aim to facilitate the restoration of brain function and/or behavior or improve it by self-regulation of brain activity (Thibault *et al* 2016). While assistive BCIs are application centered (steering of a wheelchair, communication interface) neurofeedback systems are user centered (self-regulation and restoration of specific brain patterns). Furthermore, the scope of BCI research can include non-medical applications as user state monitoring and gaming (Lécuyer *et al* 2008).

Effective BCI communication or device control based on electroencephalographic (EEG) signals – EEG-based BCI – has been demonstrated using slow cortical potentials (Birbaumer *et al* 1999, Kubler *et al* 2001, Karim *et al* 2006), brain rhythms (Pfurtscheller *et al* 1997, Treder *et al* 2011, Ono *et al* 2014, McFarland *et al* 2015) or event-related potentials (Nijboer *et al* 2008, Baek *et al* 2013, Combaz and Van Hulle 2015). The most used EEG-based BCI inputs are sensory-motor rhythms (Leeb *et al* 2013, Ge *et al* 2014, Maria *et al* 2015, Ramos-Murguialday and Birbaumer 2015) and P300 evoked potentials (Pires *et al* 2012, Amaral *et al* 2015, Lopes *et al* 2016). Usually the BCI systems design emphasizes speed because the main goal is to provide motor or communication output, but applications targeting self state control, such as enabled by

visual imagery (Banca *et al* 2015), might be useful for attentional disorders such as attention deficit hyperactivity disorder (ADHD) (Abraham *et al* 2006).

One of major goals of the current BCI research is to define novel tasks and approaches that can be used in non-motor disorders and increase the number of classes and the intrinsic number of levels of control, i.e. to increase the degrees of freedom. This would mainly allow to develop novel and more precise forms of neurofeedback. The conventional P300 paradigms generate various BCI commands allowing, for example, to move a wheelchair (Lopes *et al* 2016) or to generate a speller (Pires *et al* 2012). However, they associate commands to different stimuli presented to the subjects requiring all the time a stimulus to encode the attentional focus. BCI systems based on imagery are an alternative to the need of an external stimulus to encode the users' intention.

Human brain functions can be at least in part spatially localized, even in EEG, and thus separate commands can be encoded by taking advantage from information derived from functional modules evoking spatially distinct patterns of activity. This possibility is commonly used in BCI systems based on motor imagery, where the imagery of different motor actions (for example, leg or hand movement, right and left) produces spatially distributed brain activations (Ramos-Murguialday and Birbaumer 2015, Schlögl *et al* 2005). Although, the subjects usually receive instructions to imagine themselves performing a specific motor action without overt motor output, dependent on the exact manner of how subjects perform this task, the relative contribution of various aspects involved in motor imagery may vary and distinct neural processes may therefore be recruited.

Multiclass systems based on self-regulation of different brain rhythms combined or based on multilevel control of the same brain rhythm have already been explored. Wolpaw and McFarland suggested a multidimensional point-to-point movement control based on the combination of mu or beta rhythm amplitude modulation over the right and left sensorimotor cortices (Wolpaw and McFarland 2004). They showed that people can learn to use scalp-recorded EEG rhythms to move a cursor in two dimensions, and recently also in 3 dimensions (McFarland *et al* 2010). In another study, it was shown that self-regulation of slow cortical potentials can be reliably translated as two BCI commands (Karim *et al* 2006). More recently, a BCI study proposed an approach where participants were able to switch between modulation of alpha-band and gamma-band oscillations in the visual cortex (Salari and Rose 2013). However, for these particular

studies the users' self-regulation of one specific brain rhythm allowed only two instances of control. Furthermore, the described BCI approaches required some days of training.

In this work we aim to test the possibility of obtaining three classes of control based on evoked brain activity by pure visual motion imagery of an external actuator. Our hypothesis is that using visual imagery strategies with different number of motion alternations it is possible to achieve different patterns of brain activity modulation allowing for state related self-regulation based multiclass control. From functional magnetic resonance imaging (fMRI) studies it is known that in the visual motion perceptual domain conditions for which motion alternations occur more often lead to stronger brain activity modulations (Tootell *et al* 1998, Huk and Heeger 2002, Larsson *et al* 2006, Sousa *et al* 2016). We use the imagery of three stimulation conditions with different number of motion alternations (imagery of a static dot – no motion, imagery of a dot with two opposing motions in the vertical axis – constant motion and, imagery of a dot with four opposing motions in the vertical and horizontal axes – alternate motion) to test if using EEG it is possible to distinguish three patterns of brain activity according to the level of imagined motion alternation, as previously shown with fMRI (Sousa *et al* 2016). This would allow for the implementation of a multilevel or at least a multiclass control EEG based approach mainly depending on the applied imagery strategy irrespective of prior participant training. Furthermore, in contrast to classical motor imagery strategies this approach is not influenced by participants' movements and, in contrast to the P300 approaches does not depend on an external stimulus.

Visual imagery refers to the emergence of constructive representations and the accompanying perceptual experience without a direct external stimulus (Pearson *et al* 2015). This process plays a core role in many mental health disorders, such as ADHD, anxiety, bipolar disorder and schizophrenia, which may have therapeutic implications (Hackmann and Holmes 2004, Abraham *et al* 2006, Holmes *et al* 2007, Brewin *et al* 2010; Holmes and Mathews 2010, Banca *et al* 2015). Therefore, we expect that the present work might contribute to the discussion on feasibility of multiclass self-regulation control for implementation in BCI methods, as well as on the potential usefulness of finer control of visual imagery in mental disorders.

In 2005 Neuper and colleagues explored the potential of visual-motor imagery as a control strategy in comparison to motor imagery (Neuper *et al* 2005). They found that to improve BCI control the user training should emphasize kinesthetic experiences instead of visual representations of actions, since only kinesthetic motor imagery, but not visual-motor imagery,

resulted in detectable (versus baseline, and by a classifier) EEG changes. However, that study focused on visual-motor imagery while we focused on pure visual imagery, which might be potentially relevant for mental disorders such as the ones affecting attentional processes.

Methods

Participants

Twelve males participated in this study. On average, study participants were 28.9 years old (*SD* = 3.8 range 21-34 years). All participants were right-handed, had normal or corrected-to-normal vision and reported no medical or psychological disorders. Participants gave written informed consent prior to the EEG recording session. The procedure was approved by the Ethics Committee of the Faculty of Medicine of the University of Coimbra.

Experimental design

The experiments were composed of two interleaved sessions in the same day: visual motion stimulation and visual motion imagery. The visual stimulation paradigm was used as a guide to the visual motion imagery tasks. During the visual stimulation session, participants were asked to fixate a central cross. As illustrated on figure 1, three different conditions were used: (A) zero motion (static dot), (B) a dot moving in two opposing directions (with constant vertical orientation – along y axis, less alternation, hereinafter referred as constant motion) and (C) a dot moving in four opposing directions (horizontal and vertical orientations – along x and y axes, more alternation, hereinafter referred as alternate motion). Four second trials of a moving dot (5 deg/s) were randomly presented after each 2 seconds trial of a static dot. The distance covered by the dot was 2.5 degrees of arc. The motion conditions were repeated 60 times divided in two parts. The point size was 0.5 x 0.5 cm^2 (dot visual angle: 0.64 deg) and the stimulus was displayed at 44.5 cm from the participant at a screen of 24.1 x 18.2 cm^2. Stimulus display and imagery instructions were controlled by MATLAB (MathWorks) using the Psychophysics toolbox (Brainard, 1997).

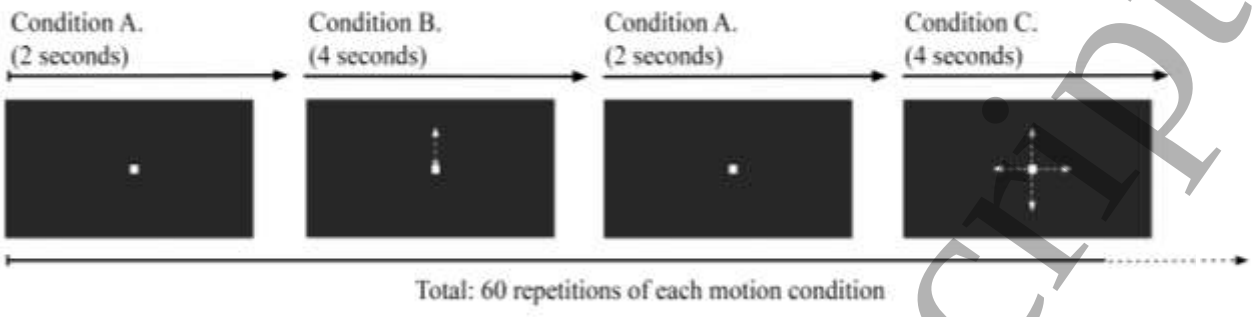

Figure 1. Stimulation conditions. (A) Static dot - static condition used as baseline to the motion conditions, (B) constant motion - moving dot alternating the direction, and (C) alternate motion - moving dot alternating the direction and the orientation. The arrows are here merely representing the dot motions. Each motion condition was repeated 60 times and randomly interleaved with the static dot condition. The duration of each motion condition was 4 seconds. Each static dot trial was presented only during 2 seconds.

In the visual motion imagery session, participants were asked to imagine the three previously presented stimulus conditions. The instruction for each imagery task was provided as an auditory cue coded as 'A', 'B' and 'C' respectively, and took one second. A beep sound was given to the participants 1.5 seconds after the beginning of each motion imagery task as a reminder of the spent imagery time.

The duration and number of repetitions of each task were equal to the stimulation session ones. The imagery session was divided in two parts intercalated with stimulation (also divided in two parts) in order to decrease fatigue effects. Participants were seated comfortably in the darkened sound-attenuating EEG recording room and, were asked to breathe steadily and to remain as still as possible. Throughout the visual imagery tasks participants were also asked to close the eyes in order to prevent sources of visual noise. Although in real life implementations people should keep their eyes open, here we prioritized the optimization of signal to noise in our design of this proof-of-concept study, as already done in other visual imagery studies (De Pisapia *et al* 2016).

Data acquisition

First, the participants scalp was cleaned using abrasive gel and then an actiCAP cap was placed on their heads. The EEG was recorded by means of a Brain Products Package (Brain Products, Germany) and sampled at a frequency of 1000 Hz. Ag/AgCl active electrodes (Brain Products), were located in 58 positions (according to the international 10-20 system with interspaced positions, figure 2), a ground electrode was located on the forehead and, two reference electrodes

were placed on the earlobes. The electrooculogram (EOG) was monitored via electrodes positioned at the standard positions (vertical and horizontal) to be used in the correction of artifacts due to blinking and eye movements. The signal was filtered between 0.1 Hz and 100 Hz and an additional 50 Hz notch filter was applied to avoid power line contamination. Electrode impedances were kept below 10 kΩ during the acquisitions.

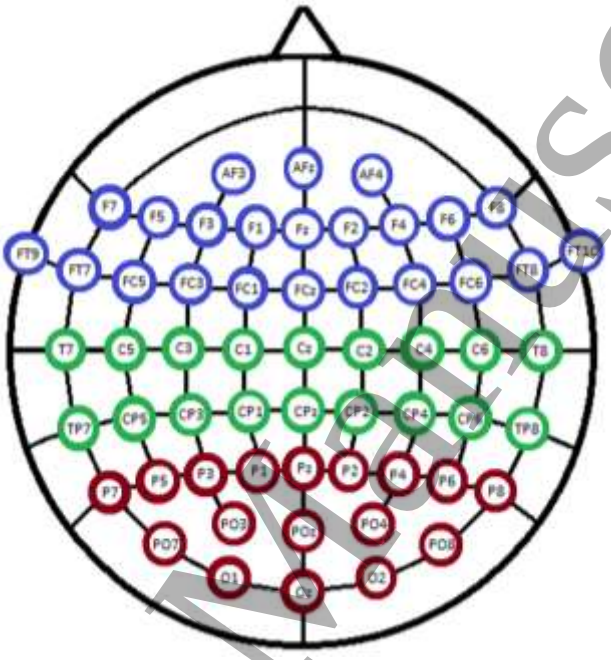

Figure 2. Layout of the EEG channel acquisition set up (58 EEG channels). The three channel clusters used in statistical data analysis are highlighted at different colors (frontal – blue, central – green, parieto-occipital – red).

Data analysis

The data analysis was performed offline using Matlab (MathWorks) and the EEGLAB toolbox (version 13.5.4b) (Delorme and Makeig 2004). The signals were re-referenced to the average signal of the earlobes channels and filtered between 0.5 Hz and 70 Hz and segmented in epochs locked to each stimulation condition/imagery task onset. Then, we applied an eye movement related artifact correction procedure based on independent component analysis (ICA) of all electrode data (including the EOG channels). Artifact components were identified using ICA and these components examined based on their correlation with the EOG electrodes and on the scalp topography (increased activity distribution) and removed from the data (Keren *et al* 2010). Signals were also corrected for possible artifacts related to body movement or muscle tension, which were marked and excluded from further analysis. After artifact rejection we were able to

keep more than 50 epochs for each stimulation condition/imagery task, except for the imagery data of one participant. For the data analysis of visual motion stimulation, we used a baseline taken from the last 500 ms of pre-stimulus time (last 500 ms of static dot condition before the motion conditions). For visual motion imagery data, the baseline was based on the last 500 ms of the static dot imagery period.

We performed time-frequency analyses of the imagery data and of the stimulation data (as a control study). Mean event-related changes in spectral power (from baseline) at each time during the epochs and at each frequency were analyzed using the event-related spectral perturbation (ERSP) method (Makeig, 1993). ERSP analyses were performed for frequencies ranging from 3 to 50 Hz for all channels by applying Morlet wavelets with incremental cycles (2 cycles at 3 Hz, up to 27 at 50 Hz) resulting in 200 time points. To visualize power changes across the frequency range, the mean baseline log power spectrum from each spectral estimate was subtracted producing the baseline-normalized ERSP. Significance of deviations from baseline power was assessed using a bootstrap method. ERSP group results were analyzed at $P = 0.05$ (Delorme and Makeig 2004).

In order to understand the main differences for specific frequency bands between stimulation conditions and between imagery tasks, the mean power of EEG signal from all channels over the 500 ms and 1500 ms of all epochs was calculated for the three stimulation conditions and for the three imagery tasks. The power spectral density (PSD) was estimated via the Welch's method which uses the Fast Fourier Transform (FFT) (Welch, 1967).

We also performed source localization of the EEG data based in sLORETA (standardized low resolution brain electromagnetic tomography) software package (Pascual-Marqui, 2002). This method employs the current density estimate given by the minimum norm solution. The localization inference is based on standardized values of the current density estimates (Pascual-Marqui *et al* 1994, Pascual-Marqui 2002). The source analysis was performed to infer about the biological significance of the most relevant frequency data.

Imagery data classification

In order to verify if the three employed imagery tasks may lead to successful achievement of three classes of control in BCI applications, we attempted to classify these classes using a reduced number of channels and features.

We used pre-processed (filtered, re-referenced and with artifact correction) trials, with one second each (from 0.5 to 1.5 of each trial). The duration of the trials used for classification was chosen to be the same to the three conditions and to not include the reminder beep. The initial 0.5 seconds after the auditory instruction cue were also excluded.

The features were extracted from a set of channels empirically chosen based on the group power spectrum per channel. The relative spectral power (RSP) of the frequency band from 7 Hz to 15 Hz was extracted from 6 EEG channels (F3, F5, FC3, FC5, C3, C5). The frequency band was chosen in order to take into account the variability in alpha activity definition across different subjects (Haegens *et al* 2014). These 6 features from 50 trials of each imagery task were normalized and then classified using a support vector machine (SVM).

As shown in previous studies (Khalighi *et al* 2013, Sousa *et al* 2015), the RSP provides some of the most relevant information from the EEG signals to classification. The RSP of each frequency-band is given by the ratio between the band spectral power and the total spectral power (Mormann *et al* 2007). The spectral power was calculated based on FFT. To avoid features in greater numeric ranges dominating those in smaller numeric ranges, each feature was independently normalized dividing its value by the difference between maximum and minimum of the feature across training trials.

The classifier was trained and tested using leave-one out cross-validation (LOOCV). The Libsvm toolbox (Chang and Lin 2011) with a sigmoid kernel was used in classification. The sigmoid degree and *C* parameter of SVM were optimized between 0 and 5 for each participant model classification. The classifier was trained and tested individually per participant. In order to characterize the trial-by-trial classification performance, some well-known measures such as balanced accuracy, sensitivity and specificity were used.

Statistical Analysis

Statistical analyses were performed to compare the group mean EEG power for the most relevant frequency bands found in the evoked brain responses during the three during the three imagery tasks and during the stimulation conditions (as a control study). The Friedman's test was applied to verify the presence of a main effect for each defined frequency band. Further, we computed pairwise comparisons for stimulation condition/imagery task per EEG channel cluster using Wilcoxon tests and applying the Dunn's correction for multiple comparisons. The EEG data

were organized in three channel clusters: frontal (anterior-frontal, frontal, fronto-temporal and fronto-central channels), central (central, centro-parietal, temporal and tempo-parietal channels) and parieto-occipital (parietal, parieto-occipital and occipital channels). Statistical analyses were performed with the IBM (Armank, NY) SPSS Statistics 22.0 software package.

Results

Visual motion stimulation

Comparing the evoked brain activation by the motion conditions to the static dot condition brain response (used as baseline) we found a significant decrease, as expected, of alpha-band power mainly in the parietal, parieto-occipital and occipital channels for visual moving stimuli conditions (figure 3).

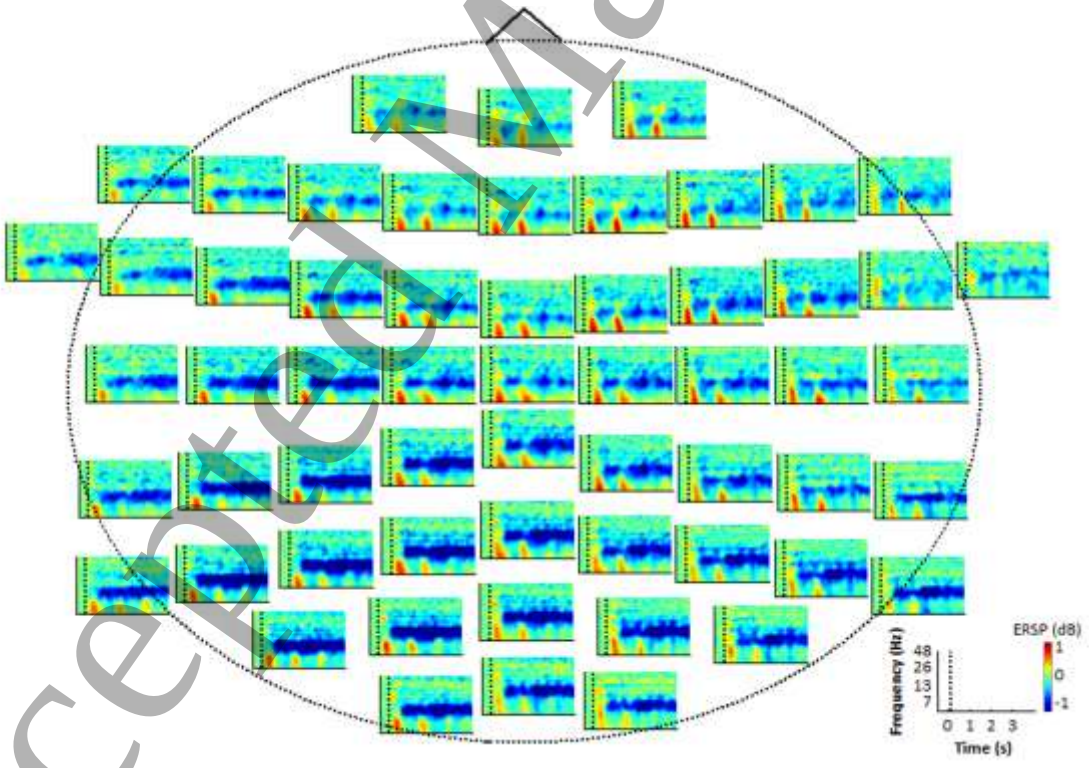

Figure 3. Brain responses to visual moving stimuli. Group event-related spectral perturbation (ERSP) for frequencies between 5 Hz and 50 Hz across entire trials (from -0.5 second to 4 seconds) pooled for moving stimuli when compared to a no-motion stimulation condition (baseline). All shown ERSP values different from zero are significant at $P = 0.05$.

For the parieto-occipital channels cluster we found statistically significant main effects for the evoked mean alpha-band power during the different stimulation conditions ($\chi_F^2(2) = 10.57$, $P = 0.005$). The peak power frequency (10 Hz) is consistent across the brain responses to the different stimulation conditions and is within the conventional alpha-band (figure 4). The alpha-band power was significantly lower during both moving stimulation conditions (constant motion – CM: $P = 0.01$; alternate motion – AM: $P = 0.02$) than during the no-motion stimulation (static dot – ST). Concerning the frontal and central channel clusters we found no significant differences. In the mean of participants and parieto-occipital cluster of channels, the power spectrum of the evoked brain activity during the constant motion stimulation and the alternate motion stimulation is similar.

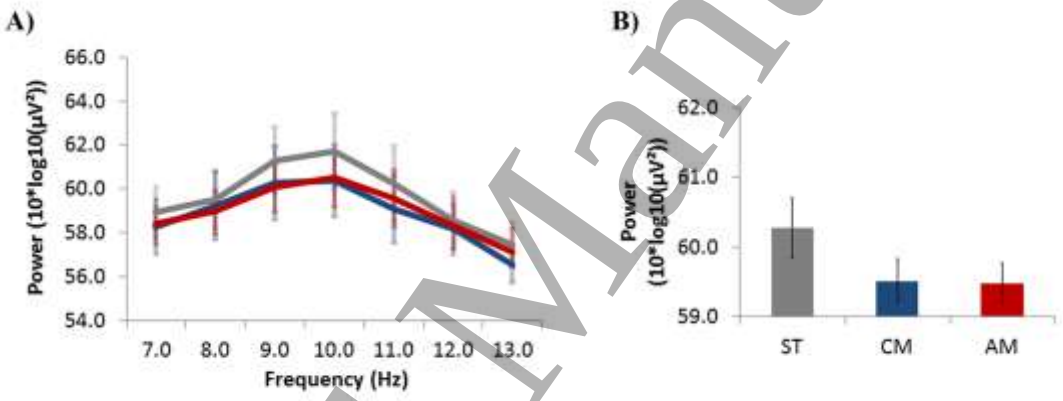

Figure 4. Group mean alpha-band power according to stimulation conditions (± standard mean error). Power spectrum of the evoked brain activity recorded in occipital channels cluster per stimulation condition (A) and its average from 8 Hz to 12 Hz (B). Color codes: red - alternate motion (AM), blue - constant motion (CM), gray - static dot (ST). The alpha-band power decreases significantly from no-motion to motion conditions (CM vs. ST, $P = 0.01$, corrected; AM vs. ST, $P = 0.02$, corrected).

Visual motion imagery

The time-frequency analyses of the visual motion imagery tasks revealed an increase of the alpha power activity when compared to the baseline (imagery of a static dot), starting after the participants received the specific imagery instruction (figure 5). This effect is mainly evident for the frontal and central EEG channels, corroborating the notion that it is a different type of alpha activity as compared to the decreasing pattern seen for real stimulation conditions (figure 3). The ERSP of both visual motion imagery conditions show some noticeable differences (see on example in supplementary figure 1). The increase of the frontal alpha signal power seems to be

more sustained during alternated visual motion imagery than during continuous visual motion imagery. Although these differences are not identified by standard statistical analysis (because they not survive correction for multiple comparisons), they suggest the potential for being separable using pattern recognition methods (see below the results). Furthermore, in some fronto-central channels we also found a decrease of the frequency power around 26 Hz during the alternated visual motion imagery. There is also a change in ERSP around 1.5 s (figure 5) that is probably resulting from the reminder beep, since they are coincident.

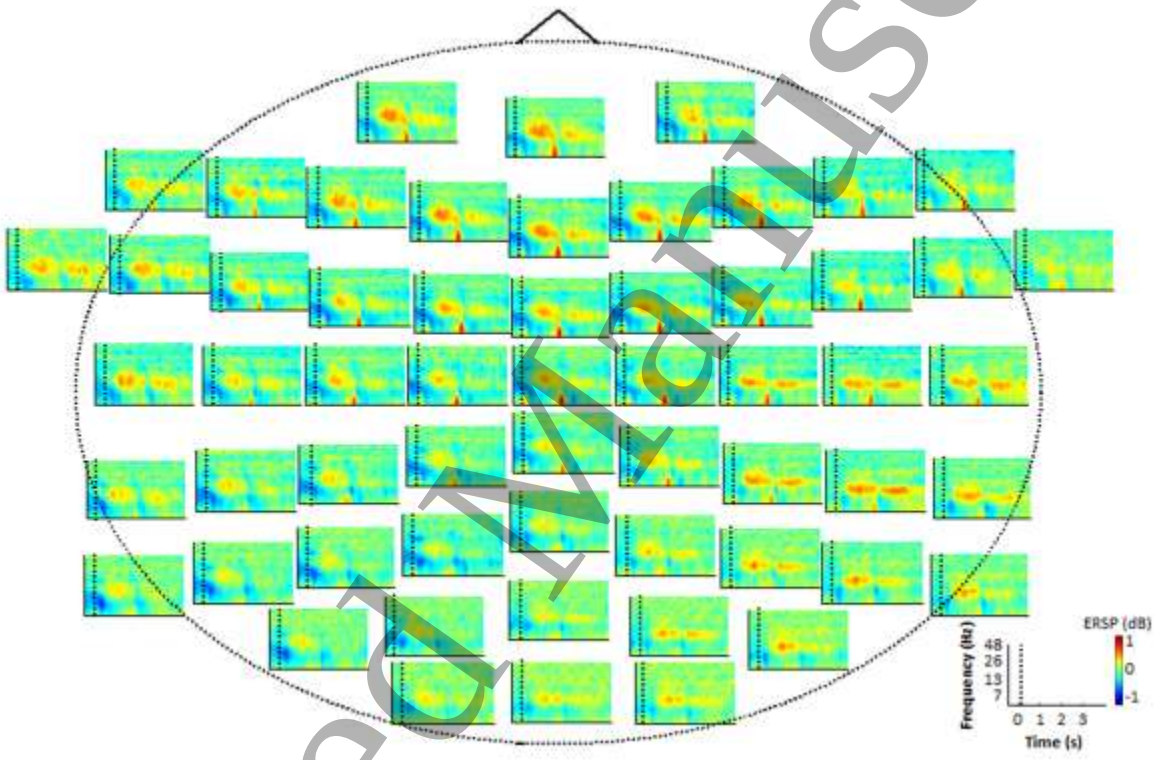

Figure 5. Brain responses to visual motion imagery. Group event-related spectral perturbation (ERSP) for frequencies between 5 Hz and 50 Hz across entire trials (from -0.5 second to 4 seconds) pooled for motion imagery tasks when compared to a no-motion imagery task (baseline). Time *0* corresponds to auditory instruction end. All shown ERSP values different from zero are significant at $P = 0.05$.

The mean alpha power (figure 6A) shows significant differences between the imagery tasks on the frontal channel cluster (χ_F^2 (2) = 13.56, P = 0.001). Post hoc tests revealed the existence of statistically significant differences between the average of alpha-band power evoked by imagery of a static dot and by constant motion imagery (P = 0.007) and between the average of alpha-band power evoked by imagery of a static dot and by the alternate motion imagery (P = 0.003). The peak power frequency (around 10 Hz) is consistent across cortical responses during the different imagery tasks. As stated above, although a classical statistical approach does not allow

for discrimination between both visual motion imagery strategies, the alpha-band power during the alternate motion imagery seems distinct from the pattern observed during constant motion imagery (mainly from 10 Hz to 12 Hz, figure 6B), suggesting that a multivariate analysis strategy based on SVM classification might be a viable approach (see below the results).

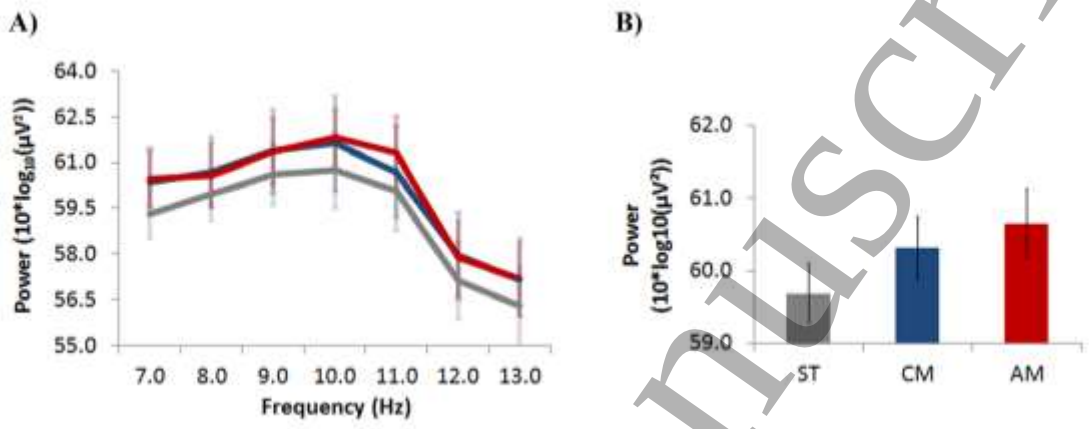

Figure 6. Group mean alpha-band power according to each imagery task (± standard mean error). Power spectrum of the evoked brain activity recorded in frontal channels cluster per imagery task (A) and its average at 10 Hz to 12 Hz for the three imagery tasks (B). The average results from 8 Hz to 12 Hz and representative individual results are presented as supplementary figure 2 and 4. Color codes: red - alternate motion imagery (AM), blue - constant motion imagery (CM), gray - static dot imagery (ST). The alpha-band power of the evoked brain activity recorded in frontal channels cluster differs significantly between the moving stimuli and the no-motion stimulus (CM vs. ST, $P = 0.007$, corrected; AM vs. ST, $P = 0.003$, corrected).

In order to understand the origin of the alpha activity increasing during the visual imagery of motion when compared to the visual imagery of a static dot, the EEG source localization for alpha-band (from 8 Hz to 12 Hz) and for two frequency sub-bands within the alpha range were examined (from 8 Hz to 10 Hz and from 10 to 12 Hz) applying the sLORETA method. The different frequency sub-bands analyzed within the alpha range were based on the notion that brain activity evoked by sensory stimulation or imaging peaks tend to differ (Klimesch 1999, Klimesch *et al* 2007). The source localization for activity evoked within this frequency-band during visual stimulation was also performed as a control. We used the comparison of visual moving stimuli (both motion conditions data combined) versus no-motion stimulus and the comparison of visual motion imagery (both visual motion imagery tasks data combined) versus no-motion visual imagery, using the data time interval from 0.5 seconds to 1.5 seconds.

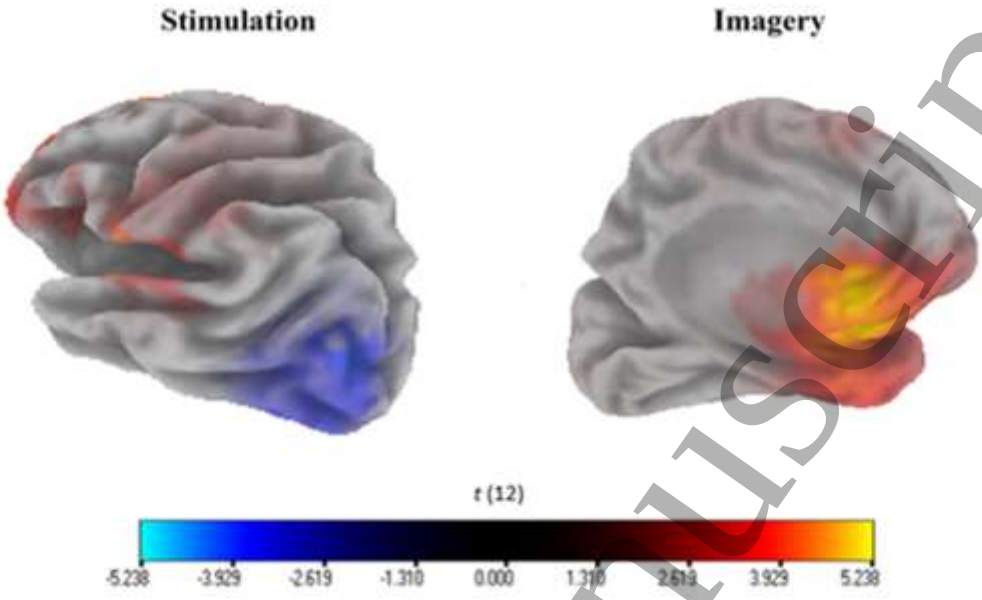

Figure 7. Source localization of the distinct alpha activity alterations during visual stimulation (control experiment) and visual imagery performed using sLORETA. Visual stimulation elicits the well-known posterior alpha desynchronization while imagery evokes anterior alpha synchronization. The source found for the decrease in alpha during visual moving stimuli, when compared to non-moving stimulus, is shown at the left panel (maximum difference at the frequency-band from 8 Hz to 10 Hz). The right panel shows the identified dominant frontal source for the increase in alpha during visual motion imagery when compared to non-motion imagery (maximum difference at the frequency-band from 10 Hz to 12 Hz). The other views of each source analysis are provided as supplementary figure 3.

The highest level of alpha activity during the visual motion imagery in relation to the imagery of a static dot was found on the frontal lobe (t = 5.24, significant at P = 0.05 for two-tailed t test) at the frequency-band from 10 Hz to 12 Hz (figure 7, right). During the visual moving stimulation the lowest recorded level of alpha activity (desynchronization) in relation to the non-moving stimulus evoked brain activity was found in the occipital lobe at the frequency-band from 8 Hz to 10 Hz (t = -4.52, significant at P = 0.05, two-tailed t test) (figure 7, left).

Visual motion imagery classification

The data were classified on trial-by-trial basis and using the relative spectral power of the frequency band from 7 Hz to 15 Hz of 6 selected EEG anterior channels (F3, F5, FC3, FC5, C3, and C5).

The results that reflect the success of distinction between each of the different combinations of classes are presented in the confusion matrix (table 1). The balanced accuracy was also

calculated per class using a one-vs-all configuration based on those results. Once we have the per-class accuracy for every class, we got the total balanced accuracy (table 2). On average the three imagery tasks were classified with 87.64 % discrimination accuracy: 88.68 % on the classification of static dot imagery, 88 % on the classification of constant motion imagery, and 86.23 % on the classification alternate motion imagery.

Table 1. Confusion matrix of the total of classified EEG trials. Classification results of 550 trials from each imagery task - static dot imagery (ST), constant motion imagery (CM) and alternate motion imagery (AM).

		Classification		
		ST	**CM**	**AM**
Imagery trials	**ST**	459	38	53
	CM	27	465	58
	AM	40	56	454

Table 2. Group **classification performance ± SEM.** Sensitivity (Sens), specificity (Spec) and balanced accuracy (bACC) are presented as the group classification performance evaluation results for the imagery of a static dot (ST), imagery of a dot with constant motion (CM) and imagery of a dot with alternate motion (AM).

	Sens	**Spec**	**bACC**
ST	83.45 ± 4.20	93.91 ± 1.41	88.68 ± 2.72
CM	84.55 ± 2.47	91.45 ± 1.96	88.00 ± 2.07
AM	82.55 ± 3.16	89.91 ± 1.93	86.23 ± 2.32
Total	**83.52 ± 2.99**	**91.76 ± 1.49**	**87.64 ± 2.24**

The mean accuracy of classification was above the chance level for all participants (group results significant at $P = 0.001$ as revealed by a 2-tailed binomial test). From the eleven tested participants, only two were classified with accuracy lower than 80 %. In the group confusion matrix, it can be seen that the best performance of the classification algorithm was in the distinction of constant motion imagery from no-motion imagery. On the other hand, the classifier presented the highest number of misclassifications in distinguishing between constant motion imagery trials and alternate motion imagery trials.

Discussion

In this study we tested the hypothesis that visual motion imagery of an external actuator can lead to different discriminable classes (at least 3) of EEG signal modulation, potentially available for BCI control. We used three visual motion imagery strategies which consisted on the imagery of three visual conditions with different number of motion alternations. We were motivated by findings showing that a different number of alternating sensory/perceptual signals (real or imagined) lead to distinct neural responses (Tootell *et al* 1998, Huk and Heeger 2002, Larsson *et al* 2006, Sousa *et al* 2016). A single-trial classification approach was tested and successfully differentiated between each of the 3 imagery strategies while with standard statistical analysis we were only able to find significant differences between the imagery of no-motion and the imagery of visual motion conditions.

Visual motion imagery evoked an anterior alpha pattern different than the visual motion stimulation: in the first case we found an increase of alpha activity in fronto-central channels while for the second case we found a decrease of alpha activity in parieto-occipital channels. In other words, different functional forms of alpha activity were found for brain responses evoked by visual motion imagery and visual motion stimulation.

It is well known that visual stimulation elicits an occipital alpha power decrease, reflecting a functional mechanism by which information is gated in visual cortex (Foxe and Snyder 2011, Klimesch *et al* 2011, Schomer and Lopes Da Silva 2011, Klimesch 2012). We found similar alpha power suppression, mainly in the parieto-occipital region, during visual motion stimulation conditions. In contrast, a significant increase of alpha activity was found on the frontal channels cluster during both visual motion imagery tasks. Some studies have suggested an increase of frontal alpha activity during high internal processing demands such as during working memory tasks (Sauseng *et al* 2005, Benedek *et al* 2011) and processes requiring imagination of stimulus sequences (Cooper *et al* 2003). According to Klimesch *et al* (2007) and Schomer and Lopes Da Silva (2011) the functional state where frontal alpha oscillations are dominant reflects a state of reduced external information processing that is referred as a 'modulation gate', and the decrease of occipital alpha power corresponds to a situation in which attention to external stimuli is enabled. Moreover, previous studies suggest that mean frontal alpha amplitudes are enhanced for more complex tasks (Cooper *et al* 2003). Thus, we suggest that the differences found between the different motion alternation imagery tasks in which concerns frontal alpha activity, with a

frequency peak above 10 Hz, can be related with the process of recovering the different visualized motion sequence conditions.

The source for the highest difference between the no-motion and motion visual imagery tasks and between no-motion and motion visual stimulation conditions differs, as expected, on the alpha sub-band frequency and location. These results are in agreement with previous studies that have shown different patterns of alpha desynchronization/synchronization subdividing the alpha frequency-band into different sub-bands (Klimesch 1999, Klimesch *et al* 2007). The source localization results for the power increase during visual motion imagery can be related with the role of frontal lobe in memory processes (Lenartowicz and McIntosh 2005). In animal studies similar observations could be reported for memory tasks involving temporally complex visual information (Gaffan and Wilson 2008).

The potential value of imagery has been explored but mostly in the motor imagery domain, i.e., imagery of motor movement visualization. Neuper and collegues had shown that visual-motor imagery did not reveal a clear spatial pattern and therefore was not prone for classification (Neuper *et al* 2005). Furthermore, they also did not find parieto-occipital alpha desynchronization during imagery. Our approach was different because we applied pure visual imagery strategies of an external actuator (an object) motion which totally distinct from motor imagery.

Although a more classical statistical approach could not discern between the visual motion imagery tasks with different number of alternations, the SVM based classification algorithm performed a successful distinction between all visual motion imagery strategies supporting the advantage of multivariate data analysis approaches (Lemm *et al* 2011). The high performance achieved by the classifier reveals potentially distinguishable brain activity patterns according to each imagery task. Therefore, our results suggest that visual motion imagery can be used to achieve multiclass control systems with the potential for being implemented in BCI applications, particularly in cases of mental disorders affecting attention, such as ADHD (Banca *et al* 2015, DeBettencourt *et al* 2015, Ordikhani-Seyedlar *et al* 2016). Yet, real-time tests need to be carried out in the future to confirm the feasibility of using our analysis approach in an online scenario. Here we prioritized the optimization of signal to noise ratios in the experimental design as an offline proof-of-concept study. In future experiments is necessary to take into account that BCI users in non-controlled environments are exposed to diverse visual stimuli. Furthermore, the

occurrence of some misclassification errors related to the differentiation between constant motion imagery and alternate motion imagery, suggest that there is room for task optimization.

Conclusion

This study provides a proof-of-concept showing that it is possible to achieve up to three classes of control based on volitional brain activity modulation using pure visual motion imagery.

Results show that the frontal alpha increased during visual motion imagery of an external actuator with distinguishable patterns of activity, as assessed by a SVM classifier, depending on the level of motion alternation of the applied imagery strategy. A 3-class classifier was learned, using only a few channels, achieving 87.64% offline single-trial accuracy, which shows the potential relevance of frontal alpha activity in imagery processes and its potential application in BCI research of mental disorders affecting attention such as ADHD.

Acknowledgements

This work was supported by the Portuguese Foundation for Science and Technology (FCT) under Ph.D. fellowships SFRH/BD/80735/2011 (TS) and SFRH/BD/78982/2011 (CA), the BRAINTRAIN project FP7-HEALTH-2013-INNOVATION-1–602186, FCT-UID/NEU/04539/2013, - COMPETE, POCI-01-0145-FEDER-007440, Bial Foundation 373/14 and the FCT project AMS HMI12: RECI/EEIAUT/0181/2012 (cofounded by COMPETE). We are also very grateful to the participants for their involvement with this study. We also thank to Gabriel Costa and Gilberto Silva for the help in offline analysis of the data.

References

Abraham A, Windmann S, Siefen R, Daum I, Güntürkün O (2006) Creative thinking in adolescents with attention deficit hyperactivity disorder (ADHD). Child Neuropsychol 12:111–123.

Amaral C, Simões M, Castelo-Branco M (2015) Neural Signals Evoked by Stimuli of Increasing Social Scene

Complexity Are Detectable at the Single-Trial Level and Right Lateralized. PLoS One 10:e0121970.

Baek HJ, Kim HS, Heo J, Lim YG, Park KS (2013) Brain-computer interfaces using capacitive measurement of visual or auditory steady-state responses. J Neural Eng 10:24001.

Banca P, Sousa T, Catarina Duarte I, Castelo-Branco M (2015) Visual motion imagery neurofeedback based on the hMT+/V5 complex: evidence for a feedback-specific neural circuit involving neocortical and cerebellar regions. J Neural Eng 12:66003.

Benedek M, Bergner S, Könen T, Fink A, Neubauer AC (2011) EEG alpha synchronization is related to top-down processing in convergent and divergent thinking. Neuropsychologia 49:3505–3511.

Birbaumer N, Ghanayim N, Hinterberger T, Iversen I, Kotchoubey B, Kübler a, Perelmouter J, Taub E, Flor H (1999) A spelling device for the paralysed. Nature 398:297–298.

Brainard DH (1997) The Psychophysics Toolbox. Spat Vis 10:433–436.

Brewin CR, Gregory JD, Lipton M, Burgess N (2010) Intrusive images in psychological disorders: characteristics, neural mechanisms, and treatment implications. Psychol Rev 117:210–232.

Chang C, Lin C (2011) LIBSVM : A Library for Support Vector Machines. ACM Trans Intell Syst Technol 2:1–39.

Chaudhary U, Birbaumer N, Ramos-Murguialday A (2016) Brain–computer interfaces for communication and rehabilitation. Nat Rev Neurol.

Combaz A, Van Hulle MM (2015) Simultaneous detection of P300 and steady-state visually evoked potentials for hybrid brain-computer interface. PLoS One 10:e0121481.

Cooper NR, Croft RJ, Dominey SJJ, Burgess AP, Gruzelier JH (2003) Paradox lost? Exploring the role of alpha oscillations during externally vs. internally directed attention and the implications for idling and inhibition hypotheses. Int J Psychophysiol 47:65–74.

De Pisapia N et al. (2016) Brain networks for visual creativity: a functional connectivity study of planning a visual artwork. Sci Rep 6.

DeBettencourt MT, Cohen JD, Lee RF, Norman KA, Turk-Browne NB (2015) Closed-loop training of attention with real-time brain imaging. Nat Neurosci 18:1–9.

Delorme A, Makeig S (2004) EEGLAB: An open source toolbox for analysis of single-trial EEG dynamics including independent component analysis. J Neurosci Methods 134:9–21.

Farwell LA, Donchin E (1988) Talking off the top of your head: toward a mental prosthesis utilizing event-related brain potentials. Electroencephalogr Clin Neurophysiol 70:510–523.

Foxe JJ, Snyder AC (2011) The role of alpha-band brain oscillations as a sensory suppression mechanism during selective attention. Front Psychol 2.

Gaffan D, Wilson CRE (2008) Medial temporal and prefrontal function: Recent behavioural disconnection studies in the macaque monkey. Cortex 44:928–935.

Ge S, Wang R, Yu D (2014) Classification of Four-Class Motor Imagery Employing Single-Channel Electroencephalography. PLoS One 9:e98019.

Hackmann A, Holmes E a (2004) Reflecting on imagery: a clinical perspective and overview of the special issue of memory on mental imagery and memory in psychopathology. Memory 12:389–402.

Haegens S, Cousijn H, Wallis G, Harrison PJ, Nobre AC (2014) Inter- and intra-individual variability in alpha peak frequency. Neuroimage 92:46–55.

Holmes EA, Arntz A, Smucker MR (2007) Imagery rescripting in cognitive behaviour therapy: Images, treatment techniques and outcomes. J Behav Ther Exp Psychiatry 38:297–305.

Holmes EA, Mathews A (2010) Mental imagery in emotion and emotional disorders. Clin Psychol Rev 30:349–362.

Huk AC, Heeger DJ (2002) Pattern-motion responses in human visual cortex. Nat Neurosci 5:72–75.

Karim A, Hinterberger T, Richter J, Mellinger J, Neumann N, Flor H, Kübler A, Birbaumer N (2006) Neural Internet: Web Surfing with Brain Potentials for the Completely Paralyzed. Neurorehabil Neural Repair 20:508–515.

Keren AS, Yuval-Greenberg S, Deouell LY (2010) Saccadic spike potentials in gamma-band EEG: Characterization, detection and suppression. Neuroimage 49:2248–2263.

Khalighi S, Sousa T, Pires G, Nunes U (2013) Automatic sleep staging: A computer assisted approach for optimal

combination of features and polysomnographic channels. Expert Syst Appl 40:7046–7059.

Klimesch W (1999) EEG alpha and theta oscillations reflect cognitive and memory performance: A review and analysis. Brain Res Rev 29:169–195.

Klimesch W (2012) Alpha-band oscillations, attention, and controlled access to stored information. Trends Cogn Sci 16:606–617.

Klimesch W, Fellinger R, Freunberger R (2011) Alpha oscillations and early stages of visual encoding. Front Psychol 2.

Klimesch W, Sauseng P, Hanslmayr S (2007) EEG alpha oscillations: The inhibition-timing hypothesis. Brain Res Rev 53:63–88.

Kubler A, Neumann N, Kaiser J, Kotchoubey B, Hinterberger T, Birbaumer NP (2001) Brain-computer communication: Self-regulation of slow cortical potentials for verbal communication. Arch Phys Med Rehabil 82:1533–1539.

Larsson J, Landy MS, Heeger DJ (2006) Orientation-selective adaptation to first- and second-order patterns in human visual cortex.

Lécuyer A, Lotte F, Reilly RB, Leeb R, Hirose M, Slater M (2008) Brain-computer interfaces, virtual reality, and videogames. IEEE Comput 41:66–72.

Leeb R, Perdikis S, Tonin L, Biasiucci A, Tavella M, Creatura M, Molina A, Al-Khodairy A, Carlson T, Millán JDR (2013) Transferring brain-computer interfaces beyond the laboratory: Successful application control for motor-disabled users. Artif Intell Med 59:121–132.

Lemm S, Blankertz B, Dickhaus T, Müller K-R (2011) Introduction to machine learning for brain imaging. Neuroimage 56:387–399.

Lenartowicz A, McIntosh AR (2005) The role of anterior cingulate cortex in working memory is shaped by functional connectivity. J Cogn Neurosci 17:1026–1042.

Lopes A, Rodrigues J, Perdigão J, Pires G, Nunes U (2016) A New Hybrid Motion Planner: Applied in a Brain-Actuated Robotic Wheelchair. IEEE Robot Autom Mag 23:82–93.

Makeig S (1993) Auditory event-related dynamics of the EEG spectrum and effects of exposure to tones. Electroencephalogr Clin Neurophysiol 86:283–293.

Maria A-VL, Antonio S-RR, A. R-MR (2015) Motor Imagery based Brain-Computer Interfaces: An Emerging Technology to Rehabilitate Motor Deficits. Neuropsychologia:1–10.

McFarland D, Sarnacki WA, R W (2015) Effects of training pre-movement sensorimotor rhythms on behavioral performance. J Neural Eng 12:66021.

McFarland DJ, Sarnacki W a, Wolpaw JR (2010) Electroencephalographic (EEG) control of three-dimensional movement. J Neural Eng 7:36007.

McFarland DJ, Wolpaw JR (2011) Brain-Computer Interfaces for Communication and Control. Commun ACM 54:60–66.

Mormann F, Andrzejak RG, Elger CE, Lehnertz K (2007) Seizure prediction: the long and winding road. Brain 130:314–333.

Neuper C, Scherer R, Reiner M, Pfurtscheller G (2005) Imagery of motor actions: Differential effects of kinesthetic and visual-motor mode of imagery in single-trial EEG. Cogn Brain Res 25:668–677.

Nijboer F, Sellers EW, Mellinger J, Jordan M a, Matuz T, Furdea A, Halder S, Mochty U, Krusienski DJ, Vaughan TM, Wolpaw JR, Birbaumer N, Kübler A (2008) A P300-based brain-computer interface for people with amyotrophic lateral sclerosis. Clin Neurophysiol 119:1909–1916.

Ono T, Shindo K, Kawashima K, Ota N, Ito M, Ota T, Mukaino M, Fujiwara T, Kimura A, Liu M, Ushiba J (2014) Brain-computer interface with somatosensory feedback improves functional recovery from severe hemiplegia due to chronic stroke. Front Neuroeng 7:19.

Ordikhani-Seyedlar M, Lebedev MA, Sorensen HBD, Puthusserypady S (2016) Neurofeedback therapy for enhancing visual attention: State-of-the-art and challenges. Front Neurosci 10.

Pascual-Marqui RD (2002) Standardized low-resolution brain electromagnetic tomography (sLORETA): technical details. Methods Find Exp Clin Pharmacol 24 Suppl D:5–12.

Pascual-Marqui RD, Michel CM, Lehmann D (1994) Low resolution electromagnetic tomography: a new method

for localizing electrical activity in the brain. Int J Psychophysiol 18:49–65.

Pearson J, Naselaris T, Holmes EA, Kosslyn SM (2015) Mental Imagery : Functional Mechanisms and Clinical Applications. Trends Cogn Sci 19.

Pfurtscheller G, Neuper C, Flotzinger D, Pregenzer M (1997) EEG-based discrimination between imagination of right and left hand movement. Electroencephalogr Clin Neurophysiol 103:642–651.

Pires G, Nunes U, Castelo-Branco M (2012) Comparison of a row-column speller vs. a novel lateral single-character speller: Assessment of BCI for severe motor disabled patients. Clin Neurophysiol 123:1168–1181.

Ramos-Murguialday A, Birbaumer N (2015) Brain oscillatory signatures of motor tasks. J Neurophysiol 7:jn.00467.2013.

Salari N, Rose M (2013) A Brain-Computer-Interface for the Detection and Modulation of Gamma Band Activity. Brain Sci 3:1569–1587.

Sauseng P, Klimesch W, Doppelmayr M, Pecherstorfer T, Freunberger R, Hanslmayr S (2005) EEG alpha synchronization and functional coupling during top-down processing in a working memory task. Hum Brain Mapp 26:148–155.

Schlögl A, Lee F, Bischof H, Pfurtscheller G (2005) Characterization of Four-Class Motor Imagery EEG Data for the BCI-Competition 2005. J Neural Eng 2:L14–L22.

Schomer D, Lopes Da Silva F (2011) Niedermeyer's Electroencephalography: Basic Principles, Clinical Applications, and Related Fields, 6th Ed. Lippincott Williams & Wilkins.

Shih JJ, Krusienski DJ, Wolpaw JR (2012) Brain-computer interfaces in medicine. Mayo Clin Proc 87:268–279.

Sousa T, Cruz A, Khalighi S, Pires G, Nunes U (2015) A two-step automatic sleep stage classification method with dubious range detection. Comput Biol Med 59:42–53.

Sousa T, Direito B, Lima J, Ferreira C, Nunes U, Castelo-Branco M (2016) Control of Brain Activity in hMT+/V5 at Three Response Levels Using fMRI-Based Neurofeedback/BCI. PLoS One 11:e0155961.

Thibault RT, Lifshitz M, Raz A (2016) The self-regulating brain and neurofeedback: Experimental science and clinical promise. Cortex 74:247–261.

Tootell RB, Hadjikhani NK, Vanduffel W, Liu AK, Mendola JD, Sereno MI, Dale AM (1998) Functional analysis of primary visual cortex (V1) in humans. Proc Natl Acad Sci U S A 95:811–817.

Treder MS, Bahramisharif A, Schmidt NM, van Gerven MAJ, Blankertz B (2011) Brain-computer interfacing using modulations of alpha activity induced by covert shifts of attention. J Neuroeng Rehabil 8:24.

Welch P (1967) The use of fast Fourier transform for the estimation of power spectra. Audio Electroacoust IEEE Trans 15:70–73.

Wolpaw JR, McFarland DJ (2004) Control of a two-dimensional movement signal by a noninvasive brain-computer interface in humans. Proc Natl Acad Sci U S A 101:17849–17854.